Contribution from the School of Chemical Sciences, University of Illinois,
505 South Mathews Avenue, Urbana, Illinois 61801

Synthetic Studies on the CpRu–PPh_3–(Se_2) System: Redox Interconversions of $Ru_2(Se_2)_2$ Cores

Jayantha Amarasekera, Eric J. Houser, Thomas B. Rauchfuss,* and Charlotte L. Stern

Received July 24, 1991

The reaction of NaSeH and $CpRu(PPh_3)_2Cl$ gave $CpRu(PPh_3)_2SeH$, while the synthesis of $(MeCp)Ru(PPh_3)_2SeH$ required the use of NMe_4SeH. The corresponding H_2Se complexes could not be prepared, as $CpRu(PPh_3)_2OTf$ failed to add H_2Se and protonation of $(MeCp)Ru(PPh_3)_2SeH$ gave $(MeCp)Ru(PPh_3)_2H_2^+$. The reaction of $CpRu(PPh_3)_2OTf$ with elemental selenium gave $[CpRu(PPh_3)_2]_2(\mu\text{-}\eta^1,\eta^1\text{-}Se_2)(OTf)_2$ (**1**). The compound **1**·PhMe·CH_2Cl_2 crystallized in the monoclinic space group $P2_1$, with $a = 15.965$ (3) Å, $b = 15.898$ (5) Å, $c = 18.406$ (4) Å, $\alpha = \gamma = 90°$, $\beta = 111.28$ (2)°, $V = 4353$ (3) Å^3, and $Z = 2$. The structure was refined to $R = 0.054$ ($R_w = 0.061$). The crystallographic studies provide evidence for Ru–Se multiple bonding but show that the Ru_2Se_2 core is not planar, unlike the core of the analogous persulfido complex. Solutions of **1** reacted further with selenium to give primarily $[CpRu(PPh_3)]_2(\mu\text{-}\eta^1,\eta^2\text{-}Se_2)_2(OTf)_2$. The analogous MeCp complex (**2**) was characterized by X-ray crystallography. It crystallizes in the triclinic space group $P\bar{1}$, with $a = 10.909$ (5) Å, $b = 13.530$ (5) Å, $c = 10.064$ (4) Å, $\alpha = 110.13$ (3)°, $\beta = 112.18$ (3)°, $\gamma = 79.62$ (3)°, $V = 1289$ (2) Å^3, and $Z = 1$. The structure was refined to $R = 0.050$ ($R_w = 0.058$). Compound **2** was reduced by Cp_2Co to give the unstable compound $[(MeCp)Ru(PPh_3)]_2(\mu\text{-}\eta^1,\eta^1\text{-}Se_2)_2$, which could be reoxidized to give **2** and which in turn thermally eliminated $SePPh_3$ to give $(MeCp)_4Ru_4Se_4$.

Introduction

Polychalcogenide ligands form complexes with all of the metals and metalloids, yet many aspects of their reaction chemistry remain unexplored.[1] Arguments have been advanced and evidence has been accumulated that polychalcogen ligands are involved in primordial chemistry,[2] the biosynthesis of metalloproteins,[3] the conversion of metals to binary chalcogenides,[4] hydrogen-transfer catalysis,[5] and energy-storage devices.[6]

Persulfido ligands in binuclear complexes exhibit a complicated structural chemistry, as this ligand can bind via a number of bonding modes.[7] Studies by several laboratories have recently demonstrated the interconversion of various μ-S_2 geometries (Scheme I).[8-13] Persulfide is a "facultative" ligand, as its coordination mode changes in response to the electronic demands of its host metal. In this paper, we examine the structural chemistry of perselenides and demonstrate the facultative character of the Se_2 ligand. This effort builds on our experience with organoruthenium sulfides.[9,14] Little previous work has appeared on ruthenium selenides,[15] and the only binary ruthenium selenide is $RuSe_2$.[16]

As with the better known persulfido group, Se_2 shows a remarkably wide variety of bonding modes. In mononuclear compounds, η^2-Se_2 coordination is observed wherein the diselenide ligand is coordinated to the metal atom in a side-on fashion. Examples of this coordination mode include $[Ir(Se_2)(dppe)_2]^+$,[17] $Os(Se_2)(CO)_2(PPh_3)_2$,[18] $Cp^*Mn(CO)_2Se_2$ ($Cp^* = C_5Me_5$),[19] and $[CpMo(CO)_2Se_2]^-$ (Cp = cyclopentadienyl).[20] The solid-state structure of $[(CO)_5W(Se_2)]_2^{2+}$ consists of two 17e $[(CO)_5W(\eta^2\text{-}Se_2)]^+$ subunits which are joined through a pair of long Se–Se bonds.[21] The μ-η^1,η^2-Se_2 coordination mode is seen in $Cp^*_2Cr_2(CO)_5(\mu\text{-}Se_2)$[22] and $[(triphos)Rh]_2(\mu\text{-}Se_2)_2^{2+}$.[23] This geometry resembles that for an alkylated $M(\eta^2\text{-}Se_2)$ moiety, e.g., $[Ir(dppe)_2Se_2Me]^{2+}$.[24] The compounds $Fe_2(CO)_6(\mu\text{-}Se_2)$,[25] $[W_2Cl_8(\mu\text{-}Se)(\mu\text{-}Se_2)]^{2-}$,[26] $Nb_4(MeCN)_4Br_6(\mu\text{-}Br)_4(\mu_2\text{-}Se_2)(\mu_4\text{-}Se)$,[27] and $(Me_2S)_2Cl_2Nb(\mu\text{-}Se_2)_2NbCl_2(SMe_2)_2$[28] feature μ-η^2,η^2-Se_2 coordination. This same geometry is proposed for $Cp^*_2Mo_2Se_4$.[29] Combinations of these bonding motifs are found in $(MeCp)_2V_2(\mu\text{-}Se)(\mu\text{-}\eta^1,\eta^1\text{-}Se_2)(\mu\text{-}\eta^2,\eta^2\text{-}Se_2)$[30] and $[V_2(\mu\text{-}\eta^2\text{-}Se_2)_2(\eta^2\text{-}Se_2)_2(\mu\text{-}\eta^1,\eta^2\text{-}Se_5)]^{2-}$.[31] *trans*-$\mu$-$\eta^1,\eta^1$-$Se_2$ bonding modes

---

(1) Draganjac, M.; Rauchfuss, T. B. *Angew. Chem., Int. Ed. Engl.* **1985**, *24*, 742. Müller, A.; Diemann, E. *Adv. Inorg. Chem.* **1987**, *31*, 89. Ansari, M.; Ibers, J. A. *Coord. Chem. Rev.* **1990**, *100*, 223. Wachter, J. *Angew. Chem., Int. Ed. Engl.* **1989**, *28*, 1613.

(2) Wächterhäuser, G. *Microbiol. Rev.* **1988**, *52*, 452.

(3) Coucouvanis, D.; Swenson, D.; Stremple, P.; Baenziger, N. C. *J. Am. Chem. Soc.* **1979**, *101*, 3392.

(4) Rauchfuss, T. B.; Ramli, E. R. *J. Am. Chem. Soc.* **1990**, *112*, 4043.

(5) Rakowski, Dubois, M. *Chem. Rev.* **1989**, *89*, 1.

(6) Jacobson, A. J. *Solid State Ionics* **1981**, *5*, 65. Alonso Vante, N.; Tributsch, H. *Nature* **1986**, *323*, 431.

(7) Müller, A.; Jaegermann, W.; Enemark, J. H. *Coord. Chem. Rev.* **1982**, *46*, 245.

(8) Bolinger, M. E.; Rauchfuss, T. B.; Rheingold, A. L. *J. Am. Chem. Soc.* **1983**, *105*, 6321.

(9) Ogilvy, A. E.; Rauchfuss, T. B. *Organometallics* **1988**, *7*, 1884.

(10) Brunner, H.; Janietz, N.; Wachter, J.; Nulser, B.; Ziegler, M. L. *J. Organomet. Chem.* **1988**, *356*, 85.

(11) Brunner, H.; Meier, W.; Wachter, J.; Guggoltz, E.; Zahn, T.; Ziegler, M. L. *Organometallics* **1982**, *1*, 1107.

(12) Brunner, H.; Merz, A.; Pfauntsch, J.; Serhadli, O.; Wachter, J.; Ziegler, M. L. *Inorg. Chem.* **1988**, *27*, 2055. Ogino, H.; Tobita, H.; Inomata, S.; Shimoi, M. *J. Chem. Soc., Chem. Commun.* **1988**, 586. Inomata, S.; Tobita, H.; Ogino, H. *Inorg. Chem.* **1991**, *30*, 3039.

(13) Weberg, R. T.; Haltiwanger, R. C.; Rakowski DuBois, M. *New J. Chem.* **1988**, *12*, 361.

(14) (a) Rauchfuss, T. B.; Rodgers, D. M. P.; Wilson, S. R. *J. Am. Chem. Soc.* **1986**, *108*, 3114. (b) Amarasekera, J.; Rauchfuss, T. B.; Rheingold, A. L. *Inorg. Chem.* **1987**, *26*, 2017. (c) Amarasekera, J.; Rauchfuss, T. B.; Wilson, S. R. *Inorg. Chem.* **1987**, *26*, 3328. (d) Amarasekera, J.; Rauchfuss, T. B.; Wilson, S. R. *J. Chem. Soc., Chem. Commun.* **1989**, 14. (e) Amarasekera, J. Rauchfuss, T. B. *Inorg. Chem.* **1989**, *28*, 3875. (f) Howard, K. E.; Rauchfuss, T. B.; Wilson, S. R. *Inorg. Chem.* **1988**, *27*, 1710. (g) Lockemeyer, J. R.; Rauchfuss, T. B.; Rheingold, A. L. *J. Am. Chem. Soc.* **1989**, *11*, 5733. (h) Houser, E. J.; Amarasekera, J.; Rauchfuss, T. B.; Wilson, S. R. *J. Am. Chem. Soc.* **1991**, *113*, 7440.

(15) Draganjac, M.; Dhingra, S.; Huang, S.-P.; Kanatzidis, M. *Inorg. Chem.* **1990**, *29*, 590.

(16) Stassen, W. N.; Heyding, R. D. *Can. J. Chem.* **1968**, *46*, 2159.

(17) Ginsberg, A. P.; Lindsell, W. E.; Sprinkle, C. R.; West, K. W.; Cohen, R. L. *Inorg. Chem.* **1982**, *21*, 3666.

(18) Farrar, D. H.; Grundy, K. R.; Payne, N. C.; Roper, W. R.; Walker, A. *J. Am. Chem. Soc.* **1979**, *101*, 6577.

(19) Herberhold, M.; Reiner, D.; Thewalt, U. *Angew. Chem., Int. Ed. Engl.* **1983**, *22*, 1000.

(20) Adel, J.; Weller, F.; Dehnicke, K. *J. Organomet. Chem.* **1988**, *347*, 343.

(21) (a) Belin, C.; Makani, T.; Rozière, J. *J. Chem. Soc., Chem. Commun.* **1985**, 118. (b) Collins, M. J.; Gillespie, R. J.; Kolis, J. W.; Sawyer, J. F. *Inorg. Chem.* **1986**, *25*, 2057.

(22) Herrmann, W. A.; Rohrmann, J. *Chem. Ber.* **1986**, *119*, 1437.

(23) Bianchini, C.; Mealli, C.; Meli, A.; Sabat, M. *J. Am. Chem. Soc.* **1985**, *107*, 5317.

(24) Hoots, J. E. Rauchfuss, T. B. *Inorg. Chem.* **1983**, *22*, 2806.

(25) Campana, C. F.; Lo, F. Y.-K.; Dahl, L. F. *Inorg. Chem.* **1979**, *18*, 3060.

(26) Drew, M. G. B.; Fowles, G. W. A.; Page, E. M.; Rice, D. A. *J. Am. Chem. Soc.* **1979**, *101*, 5827.

(27) Benton, J.; Drew, M. G. B.; Rice, D. A. *J. Chem. Soc., Chem. Commun.* **1981**, 1241.

(28) Drew, M. G. B.; Rice, D. A.; Williams, D. M. *J. Chem. Soc., Dalton Trans.* **1984**, *1087*.

(29) Brunner, H.; Wachter, J.; Wintergerst, H. *J. Organomet. Chem.* **1985**, *235*, 77.

(30) Rheingold, A. L.; Bolinger, C. M.; Rauchfuss, T. B. *Acta Crystallogr.* **1986**, *C42*, 1878.

(31) Chau, C.-N.; Wardle, R. W. M.; Ibers, J. A. *Inorg. Chem.* **1987**, *26*, 2740.

0020-1669/92/1331-1614$03.00/0

Scheme I

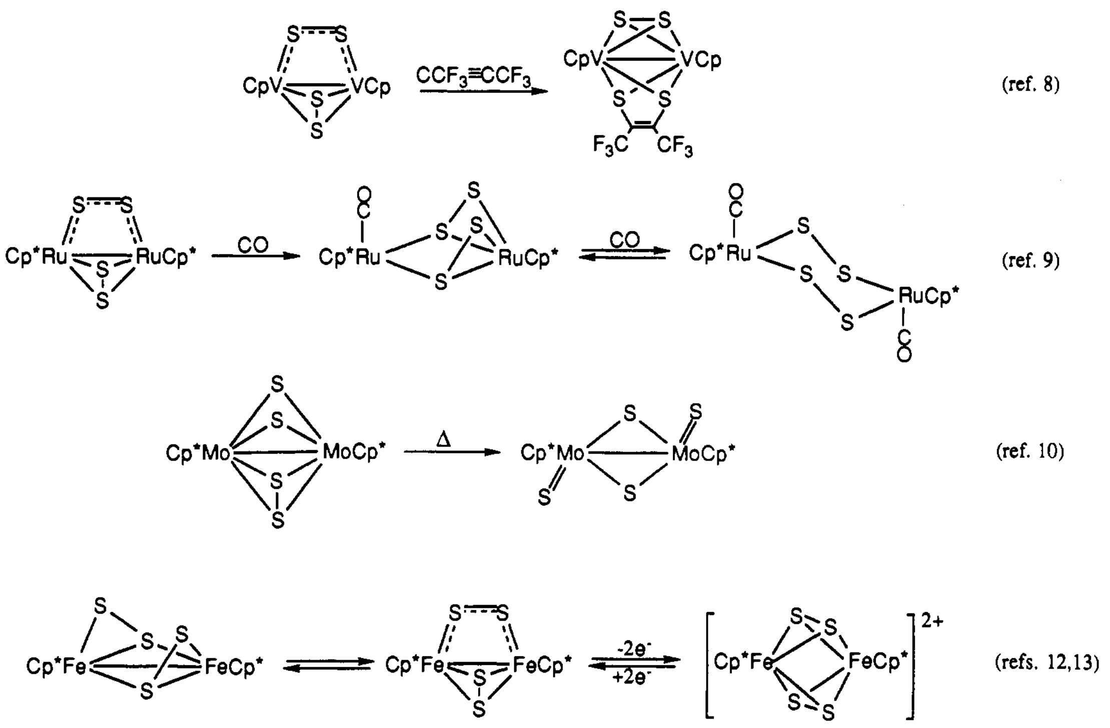

Table I. Selected Bond Distances (Å) and Angles (deg) in [CpRu(PPh$_3$)$_2$]$_2$Se$_2$(OTf)$_2$·CH$_2$Cl$_2$·PhMe

		Distances			
Ru1–Se1	2.341 (2)	Ru2–Se2	2.377 (2)	Se1–Se2	2.265 (2)
Ru1–P1	2.384 (4)	Ru1–P2	2.352 (4)	Ru2–P3	2.344 (4)
Ru2–P4	2.366 (4)	Ru1–Cp1	1.89 (1)	Ru2–Cp2	1.90 (1)
		Angles			
Se1–Ru1–P1	102.33 (10)	Se1–Ru1–P2	86.19 (10)	Se1–Ru1–Cp1	122.9 (4)
P1–Ru1–Cp1	118.5 (4)	P1–Ru1–P2	97.3 (1)	P2–Ru1–Cp1	122.7 (4)
Se2–Ru2–P3	85.9 (1)	Se2–Ru2–P4	95.9 (1)	Se2–Ru2–Cp2	126.5 (4)
P3–Ru2–P4	101.9 (1)	P3–Ru2–Cp2	121.9 (4)	P4–Ru2–Cp2	117.7 (5)
Ru1–Se1–Se2	112.94 (8)	Ru2–Se2–Se1	109.20 (8)		

have been suggested for [CpMn(CO)$_2$]$_2$Se$_2$[32] and the electron-precise [CpFe(CO)$_2$]Se$_2$.[33]

Results

(C$_5$H$_4$R)Ru(PPh$_3$)$_2$SeH. The complex CpRu(PPh$_3$)$_2$SeH is formed in good yields by slurrying CpRu(PPh$_3$)$_2$Cl and excess NaSeH in hot methanol. This neutral yellow-brown air-sensitive material is soluble in polar organic solvents. Its ^{1}H NMR spectrum shows a single Cp resonance and a phenyl multiplet along with the Se*H* resonance, which appears as a triplet at −5.9 ppm upfield of TMS (J_{PH} = 7 Hz). The ^{31}P{^{1}H} NMR spectrum of this complex consists of a single line at 44.7 ppm downfield of the 85% H$_3$PO$_4$ standard. It is interesting that the corresponding reaction of NaSeH and (MeCp)Ru(PPh$_3$)$_2$Cl is very slow. We have found however that this latter reaction proceeds well using (NMe$_4$)SeH.

Unlike the case of the CpRu(PPh$_3$)$_2$SH system, we were unable to prepare [CpRu(PPh$_3$)$_2$(SeH$_2$)]$^+$ either by protonation of CpRu(PPh$_3$)$_2$SeH with trifluoromethanesulfonic acid (HOTf) or by reaction of CpRu(PPh$_3$)$_2$OTf[34] with H$_2$Se. In order to probe this reaction more thoroughly, we turned to the analogous MeCp complexes because previous work had shown that the H$_2$S complex was more thermally robust than the Cp analogue. Treatment of a dichloromethane solution of (MeCp)Ru(PPh$_3$)$_2$SeH with HOTf afforded ~60% yield of the dihydride [(MeCp)Ru(PPh$_3$)$_2$H$_2$]$^+$, which was identified by ^{1}H and ^{31}P{H} NMR measurements.[35] This dehydrogenation does not proceed via [CpRu(PPh$_3$)$_2$]$_2$Se$_2$$^{2+}$ (discussed below), since the latter does not react with hydrogen.

[CpRu(PPh$_3$)$_2$]$_2$Se$_2$$^{2+}$. The complex [CpRu(PPh$_3$)$_2$]$_2Se_2(OTf)_2$ (**1**) forms in good yields from the reaction of red selenium with a dichloromethane solution of CpRu(PPh$_3$)$_2$OTf. This yellow-brown air stable material is soluble in polar solvents. The positive-ion fast atom bombardment (FAB) spectrum of the compound shows envelopes of peaks corresponding to [CpRu(PPh$_3$)$_2$]$_2$Se$_2$$^+$ and several of its fragments. Its ^{1}H and ^{31}P NMR spectra are indicative of a diamagnetic and centrosymmetric compound. The optical spectrum of **1** is dominated by a low-energy absorption at 790 nm (ϵ = 8.18 × 10^3 M^{-1} cm^{-1}) in methylene chloride solutions. A similar low-energy absorption band at 718 nm (ϵ = 3.2 × 10^4 M^{-1} cm^{-1}) was observed for [CpRu(PPh$_3$)$_2$]$_2$S$_2$$^{2+}$ and was assigned to transitions involving the Ru$_2$S$_2$ core.[14c]

The cyclic voltammogram of **1** in dichloromethane at a Pt electrode shows a reversible wave at 300 mV and a quasi-reversible wave at −680 mV vs Ag/AgCl. Coulometric measurements at −50 mV indicated the 300-mV wave is associated with a 1e/2Ru reduction.

In the crystal, each ruthenium atom in **1** is coordinated to a Cp ring, two triphenylphosphine groups, and one end of a μ-η^1,η^1-Se$_2$ unit, giving a pseudooctahedral coordination (Figure 1).

---

(32) Herberhold, M.; Reiner, D.; Zimmer-Gasser, B.; Schubert, U. *Z. Naturforsch.* **1980**, *35B*, 1281.

(33) Herrmann, W. A.; Rohrmann, J.; Herdtweck, E.; Hecht, C.; Ziegler, M. L.; Serhadli, O. *J. Organomet. Chem.* **1986**, *314*, 295.

(34) Amarasekera, J.; Rauchfuss, T. B.; Wilson, S. R. *J. Am. Chem. Soc.* **1988**, *110*, 2332.

(35) Conroy-Lewis, F. M.; Simpson, S. J. *J. Chem. Soc., Chem. Commun.* **1987**, 1675. We had observed formation of small amounts of metal hydrides in the reaction of [CpRu(PPh$_3$)$_2$SH$_2$]$^+$ and CpRu(PPh$_3$)$_2$OTf; see ref 14e.

Table II. Selected Bond Distances (Å) and Angles (deg) for the Centrosymmetric Cation in $[(MeCp)Ru(PPh_3)]_2(\mu\text{-}Se_2)_2(OTf)_2$

		Distances			
Ru–Se1	2.473 (1)	Ru–Se1	2.556 (1)	Ru–Se2	2.518 (1)
Se1–Se2	2.279 (1)	Ru–P	2.407 (3)		
		Angles			
Se1–Ru–Se1	76.96 (4)	Se1–Ru–Se2	98.13 (5)	Se1–Ru–P	84.82 (8)
Se1–Ru–P	126.32 (8)	Ru–Se1–Se2	114.15 (5)	Se1–Ru–Se2	53.38 (4)
Se2–Ru–P	80.71 (8)	Ru–Se2–Se1	64.16 (4)	Ru–Se1–Se2	62.46 (4)
Ru–Se1–Ru	103.04 (5)				

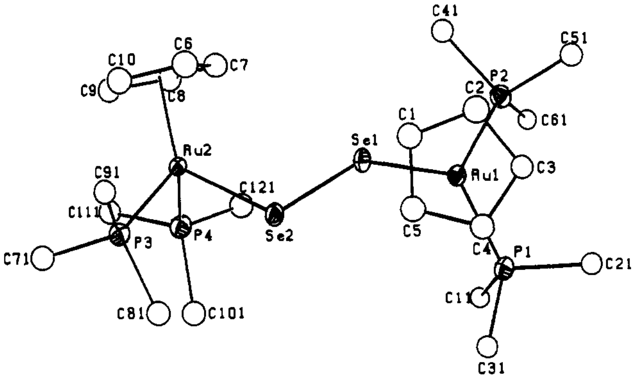

Figure 1. ORTEP diagram of the cation in $[CpRu(PPh_3)_2]Se_2(OTf)_2$ with thermal ellipsoids drawn at the 35% probability level. For the sake of clarity, only the ipso phenyl carbon atoms are shown.

The molecule possesses no crystallographic symmetry. Unlike the core of its sulfur analogue, the Ru_2Se_2 core is nonplanar with a Ru–Se–Se–Ru dihedral angle of 159.68 (7)°. Bond distances and angles are listed in Table I. In other $\mu\text{-}\eta^1,\eta^1\text{-}Se_2$ complexes, the $M_2(Se_2)$ units are cisoid, since the metals are constrained by M–M bonds. The Se–Se distance of 2.265 (2) Å lies between a Se=Se double bond (2.19 Å)[36] and a Se–Se single bond (Se_8, 2.34 Å).[37] The Se–Se bond distance in the $\{[(C_6H_5)_3P]_2CSe\}_2^{2+}$ cation, which features a *trans*-$\eta^1,\eta^1\text{-}Se_2$ group, is 2.492 (2) Å.[38] The Se–Se bond distance in **1** corresponds to an approximate bond order of 1.4 according to the bond order/distance correlation proposed by Dahl;[25] however, available reference compounds are so structurally diverse that correlations are difficult. The Ru–Se bond distances of 2.377 (2) and 2.341 (2) Å are short compared to those in the mineral $RuSe_2$ (2.44 Å).[16] They are more comparable to the average Ru–Se equatorial distance of 2.322 (6) Å observed for the 14e complex $Ru(SeC_6H\text{-}2,3,5,6\text{-}Me_4)_4(CH_3CN)$.[39]

$[(RC_5H_4)Ru(PPh_3)]_2Se_4(OTf)_2$. The reaction of excess red selenium with a dichloromethane solution of $(MeCp)Ru(PPh_3)_2OTf$ results in formation of an air-stable, red-brown compound analyzing as $[(MeCp)Ru(PPh_3)]_2Se_4(OTf)_2$ (**2**). Aside from the phenyl resonances, the ^1H NMR spectrum of **2** consists of three $CH_3C_5H_4$ signals in the ratio 2:1:1 and one methyl singlet. This indicates equivalent MeCp groups in a molecule with only rotational symmetry. Its $^{31}P\{^1H\}$ NMR spectrum consists of one signal at 31.28 ppm. Compound **2** was further characterized by FABMS. The Cp analogue of **2**, $[CpRu(PPh_3)]_2Se_4(OTf)_2$, was observed as only a minor product in the synthesis of **1** from $CpRu(PPh_3)_2OTf$ and red selenium. Indeed, solutions of **1** were found to react slowly with red selenium to give the Cp analogue of **2**.

A crystallographic study showed that each ruthenium atom in **2** is coordinated to a MeCp ring, a PPh_3 group, and three selenium atoms (Figure 2). The two $(MeCp)Ru(PPh_3)Se_2$ subunits in the structure are related by a crystallographic inversion center. Two selenium atoms, one from each of the two Se_2 units, bridge the two ruthenium centers, forming an Ru_2Se_2 ring. Similar M_2E_4 groups with $\eta^1,\eta^2\text{-}E_2$ (E = S, Se) ligands are found in $[(triphos)Rh]_2(Se_2)_2^{2+}$,[23] $Ti_2Se_8^{2-}$,[40] $Cp^*{}_2Co_2S_4$,[41] $[Mo_4(NO)_4(S_2)_5S_3]^{4-}$,[42] $Cp_2Fe_2(S_2)_2(CO)$,[43] $[MoFe_3S_6(CO)_6]^{2-}$,[44] and $[Mo_2Fe_6S_8(S_2)_2(SC_6H_4Br)_6]^{4-}$.[45] The Se–Se bond distance in **2** is 2.279 (1) Å, only slightly longer than that in **1**. Ru–Se bond distances, 2.473 (1) and 2.556 (1) Å, are, however, substantially longer than those in **1** (2.377 (2) and 2.341 (2) Å). The Ru–Ru distance of 3.937 (1) Å is nonbonding.

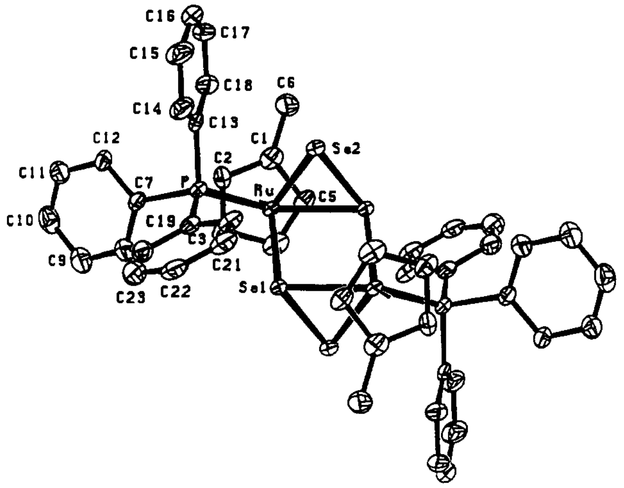

Figure 2. ORTEP diagram of the cation in $[(MeCp)Ru(PPh_3)]_2(Se_2)_2(OTf)_2$ with thermal ellipsoids drawn at the 35% probability level.

$[(MeCp)Ru(PPh_3)]_2Se_4$. The cyclic voltammogram of an acetonitrile solution of **2** at a Pt electrode shows two overlapping reversible reduction waves centered at 360 and 195 mV and a quasi-reversible wave at −1100 mV vs Ag/AgCl. The first two waves are associated with sequential 1e reductions of **2**. We found that **2** is readily reduced in solution by Cp_2Co to give an air-stable green powder formulated as $[(MeCp)Ru(PPh_3)]_2Se_4$. This complex is very poorly soluble in organic solvents but it is slightly soluble in CS_2, indicating charge neutrality. The thermal instability of its solutions interfered with purification efforts, and its characterization rests on its spectroscopy, electrochemistry, and chemical reactivity. The ^1H NMR spectrum of $[(MeCp)Ru(PPh_3)]_2Se_4$ shows two peaks for $CH_3C_5H_4$, indicating a symmetric molecule (for **2** we observe three $CH_3C_5H_4$ signals in the ratio 1:1:2). Oxidation of this green compound with Ph_3CBF_4 gives a good yield of $[(MeCp)Ru(PPh_3)]_2(Se_2)_2(BF_4)_2$. In refluxing benzene suspension, the neutral tetraselenide converts to the cubane cluster $(MeCp)_4Ru_4Se_4$. The electrochemical and spectro-

---

(36) Wells, A. F. *Structural Inorganic Chemistry*, 4th ed.; Clarendon: Oxford, England, 1975; p 521.

(37) Foss, O.; Janickis, V. *J. Chem. Soc., Chem. Commun.* **1977**, 834.

(38) Schmidbaur, H.; Zybill, C. E.; Neugebauer, D. *Angew. Chem., Int. Ed. Engl.* **1983**, *22*, 156.

(39) Millar, M. M.; O'Sullivan, T.; de Vries, N.; Koch, S. A. *J. Am. Chem. Soc.* **1985**, *107*, 3714.

(40) Kang, D.; Ibers, J. A. *Inorg. Chem.* **1988**, *27*, 549.

(41) Brunner, H.; Janietz, N.; Meier, W.; Sergeson, G.; Wachter, J.; Zahn, T.; Ziegler, M. L. *Angew. Chem., Int. Ed. Engl.* **1985**, *24*, 1060; *Angew. Chem.* **1985**, *97*, 1056. See also: Brunner, H.; Janietz, N.; Meier, W.; Wachter, J.; Herdtweck, E.; Herrmann, W. A.; Serhadli, O.; Ziegler, M. L. *J. Organomet. Chem.* **1988**, *347*, 237.

(42) Müller, A.; Eltzner, W.; Mohan, N. *Angew. Chem., Int. Ed. Engl.* **1979**, *18*, 168.

(43) Chanaud, H.; DuCourant, A. M.; Giannotti, C. *J. Organomet. Chem.* **1980**, *190*, 201.

(44) Kovacs, J. A.; Bashkin, J. K.; Holm, R. H. *Polyhedron* **1987**, *6*, 1445.

(45) Kovacs, J. A.; Bashkin, J. K.; Holm, R. H. *J. Am. Chem. Soc.* **1985**, *107*, 1784.

Scheme II

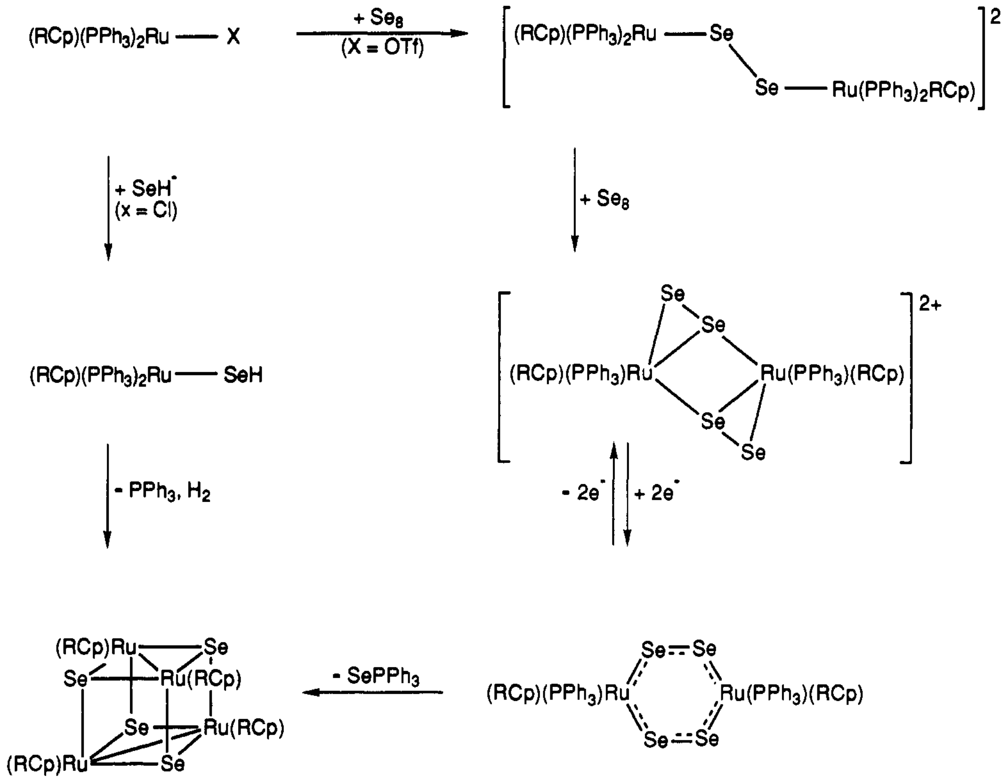

scopic properties of this cluster compound are discussed in a separate report.[46]

The cyclic voltammogram of the neutral tetraselenide (CH$_2$Cl$_2$ solution) very closely matches that of **2**, with overlapping reversible oxidation waves at 165 and 328 mV. Similarly, the sulfur analogue of this neutral tetraselenide, [(MeCp)Ru(PPh$_3$)]$_2$S$_4$, exhibits a single reversible oxidation at 75 mV.

Discussion

The reaction chemistry described in this report is shown in Scheme II. The first difference between the sulfur and selenium derivatives of the (RCp)Ru–PPh$_3$ systems is the instability of [(RCp)Ru(PPh$_3$)$_2$(SeH$_2$)]$^+$. Attempts to prepare this compound from H$_2$Se were unsuccessful, while the protonation of (RCp)Ru(PPh$_3$)$_2$SeH gave the dihydride. While it is unclear if the initial site of protonation is the metal or the Se atom, the dehydrogenation almost certainly proceeds via [(RCp)Ru(PPh$_3$)$_2$(H)(SeH)]$^+$. This hydrogen-transfer reaction would be facilitated by the fact that H$_2$Se is a stronger acid than H$_2$S ($K_a = 2 \times 10^{-4}$ vs 1×10^{-7}).[47] Since H$_2$Se is unstable with respect to H$_2$ and selenium,[48] the dehydrogenation of H$_2$Se could be made catalytic, although this was not observed.

On the basis of our work with [CpRu(PPh$_3$)$_2$]$_2$S$_2$$^{2+}$, we anticipated that its selenium analogue would be stabilized via a planar *trans*-Ru$_2$E$_2$ core. This delocalized structure may apply to **1**, although the Ru$_2$Se$_2$ unit is skewed from planarity by 20°. There are short Ru–Se and Se–Se bond distances, which indicate appreciable π-bonding between each of these atoms. In addition to the structural results, electrochemical measurements show that the μ-Se$_2$ ligand is less capable of stabilizing Ru(III) than μ-S$_2$: **1** is more easily reduced (by 120 mV) than [CpRu(PPh$_3$)$_2$]$_2$S$_2$$^{2+}$.[14c]

In this project we were able to interconvert two types of Ru$_2$(Se$_2$)$_2$ core structures by oxidation/reduction reactions. The oxidized product, [(MeCp)Ru(PPh$_3$)]$_2$(Se$_2$)$_2$$^{2+}$, was identified by spectroscopic and crystallographic methods. The structure of the reduced product, [(MeCp)Ru(PPh$_3$)]$_2$Se$_4$, was assigned on the basis of spectroscopic and electrochemical evidence and its conversion to (MeCp)$_4$Ru$_4$Se$_4$ and by analogy to the well-characterized compound [(MeCp)Ru(PPh$_3$)]$_2$(μ-S$_2$)$_2$.[14b]

A self-consistent scheme of electron accountancy rationalizes the structures of bridging perchalcogen ligands. If the metals are assigned 18e configurations, μ-η^2,η^2-S$_2$ (or -Se$_2$) and μ-η^2,η^1-S$_2$ (-Se$_2$) moieties are required to function as net 6e and 4e donors, respectively. As illustrated in our recent work, μ-η^1,η^1-S$_2$ (-Se$_2$) ligands are usually net 3e or 4e donors, the ambiguity arising because of the variable degree of metal chalcogen π-bonding as reflected in M–E distances. Illustrative of this effect, [(MeCp)Ru(PPh$_3$)]$_2$(μ-S$_2$)$_2$ can be described by two resonance structures[14b] and [CpRu(PPh$_3$)$_2$]$_2$S$_2$^{z} exists in two stable oxidation states:[14c]

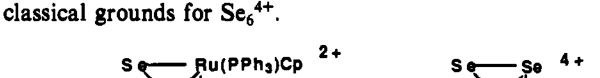

By combining these bonding modes, it can be seen that (μ-E$_2$)$_2$ can "provide" as many as 12e and as few as 6e for metal–E$_2$ bonding (Scheme III). In the absence of M–E π-bonding, the (μ-E$_2$)$_2$ unit serves as a 4e donor set.

Scheme III is also consistent with the transformations reported for complexes of the type [(C$_5$Me$_5$)MS$_2$]$_2$ (M = Fe, Ru) and [(C$_5$Me$_5$)RuS$_2$]$_2$(CO)$_x$. Finally, the structure of [(RCp)Ru(PPh$_3$)]$_2$(Se$_2$)$_2$$^{2+}$ can be related to the structure predicted on classical grounds for Se$_6$$^{4+}$.

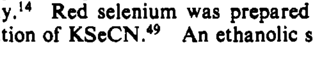

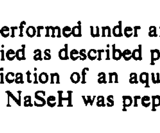

Experimental Section

Materials and Methods. All reactions were performed under an atmosphere of purified nitrogen. Solvents were dried as described previously.[14] Red selenium was prepared by acidification of an aqueous solution of KSeCN.[49] An ethanolic solution of NaSeH was prepared

---

(46) Houser, E. J.; Amarasekera, J.; Rauchfuss, T. B.; Wilson, S. R. To be submitted for publication.

(47) Rauchfuss, T. B. In *The Chemistry of Organic Selenium and Tellurium Compounds*; Patai, S., Ed.; Wiley: New York, 1987; Vol. 2, p 340.

(48) Shriver, D. F.; Adkins, P. W.; Langford, C. H. *Inorganic Chemistry*; Freeman: New York, 1990; p 279.

Scheme III

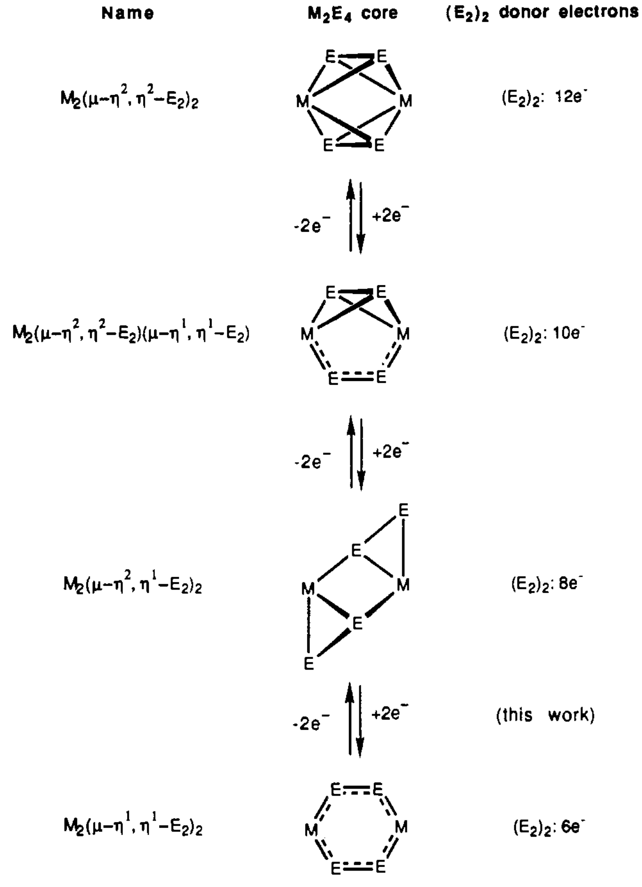

by the reaction of gray selenium and $NaBH_4$[50] and the solid product precipitated using ether. NMR measurements were made on a GE QE-300 instrument (^1H), operating at 300 MHz, and a GE GN-300 instrument (^{31}P), operating at 300 MHz. In reporting NMR data, we use the following abbreviations: s (singlet), d (doublet), t (triplet), and m (multiplet). Cyclic voltammetric data were measured on a Bioanalytical Systems BAS 100 electrochemical analyzer using platinum working and auxiliary electrodes and a Ag/AgCl reference electrode. Tetrabutylammonium hexfluorophosphate (TBAHFP) was used as a supporting electrolyte (0.1 M solution).

$CpRu(PPh_3)_2SeH$. A slurry of 0.50 g of $CpRu(PPh_3)_2Cl$ (0.69 mmol) and 0.15 g of NaSeH (1.45 mmol) in 40 mL of methanol was refluxed for 18 h. After being cooled to room temperature, the slurry was filtered and the yellow-brown microcrystalline product was collected and washed with methanol. The product was recrystallized from toluene/methanol. Yield: 0.35 g (0.45 mmol, 65%). Anal. Calcd for $C_{41}H_{36}P_2RuSe$: C, 63.89; H, 4.67; Se, 10.28. Found: C, 63.55; H, 4.57; Se, 10.92. ^1H NMR (C_6D_6): 6.9–7.5 (m, 30 H), 4.28 (s, 5 H), −5.90 ppm (t, J_{PH} = 7 Hz, 1 H). $^{31}P\{^1H\}$ NMR (toluene/C_6D_6): 44.74 ppm.

$(Me_4N)SeH$. A 30-mL aliquot of 20% methanolic $(Me_4N)OH$ (58.1 mmol) was deaerated and treated with a slow purge of H_2Se for 15 min, resulting in a light red solution. This solution was concentrated and diluted with 30 mL of diethyl ether, giving an off-white solid and a light red supernatant. The mixture was filtered, and the solid was washed with diethyl ether. The product was recrystallized by dissolution in methanol, followed by the addition of Et_2O. Yield: 6.8 g (76%). Anal. Calcd for $C_4H_{13}NSe$: C, 31.17; H, 8.50; N, 9.09; Se, 51.24. Found: C, 31.05; H, 8.55; N, 9.16; Se, 51.05.

$(MeCp)Ru(PPh_3)_2SeH$. A slurry of 0.50 g of $(MeCp)Ru(PPh_3)_2Cl$ (0.67 mmol) and 0.20 g of $(Me_4N)SeH$ (1.30 mmol) in 40 mL of methanol was refluxed for 2 h. After being cooled to room temperature, the slurry was filtered and the dark orange microcrystalline product was washed with methanol. The product was recrystallized by dissolution in toluene, followed by the addition of methanol. Yield: 0.30 g (57%). Anal. Calcd for $C_{42}H_{38}P_2RuSe$: C, 64.28; H, 4.88. Found: C, 63.99; H, 4.93. ^1H NMR (C_6D_6): 7.0–7.5 (m, 30 H), 4.03 (m, 2 H), 3.73 (m, 2 H), 2.1 (s, 3 H), −5.74 ppm (t, 1 H).

Reaction of $(MeCp)Ru(PPh_3)_2SeH$ with HOTf. In an NMR tube, 0.070 g of $(MeCp)Ru(PPh_3)_2SeH$ (0.0892 mmol) in ca. 0.7 mL of CD_2Cl_2 was treated with 8.0 μL of HOTf (0.090 mmol), resulting in an immediate color change from orange-red to brown. A 15-μL amount of the standard, $(C_6H_5)_2CH_2$ (0.089 mmol), was then added, and the product was identified by ^1H and $^{31}P\{^1H\}$ NMR spectroscopy as $[(MeCp)Ru(PPh_3)_2(H)_2]OTf$ (~60% yield). Selenium-containing products were not identified.

Attempted Reaction of $(MeCp)Ru(PPh_3)_2(OTf)$ with H_2Se. A solution of $(MeCp)Ru(PPh_3)_2(OTf)$ in CD_2Cl_2 (NMR tube) was purged with H_2Se (δ = −0.92 ppm). After 30 min, the ^1H NMR spectrum showed no change.

$[CpRu(PPh_3)_2]_2Se_2(OTf)_2 \cdot 2CH_2Cl_2$. Solid AgOTf, 0.075 g (0.28 mmol), was added to a solution of 0.20 g (0.26 mmol) of $CpRu(PPh_3)_2Cl$ in 20 mL of CH_2Cl_2. This solution was stirred for 3 h and filtered. To the filtrate was added 0.174 g (0.27 mmol) of red selenium powder, and the slurry was stirred for 12 h. The mixture was filtered in air, and the filtrate was concentrated to half-volume and diluted with ether. The yellow-brown precipitate was washed with ether and dried in vacuo. Yield: 0.160 g (70%). ^1H NMR (acetone-d_6): 7.1–7.6 (m, 60 H), 5.32 (s, CH_2Cl_2), 5.18 ppm (s, 10 H). $^{31}P\{^1H\}$ NMR ($CH_2Cl_2/CDCl_3$): 39.30 ppm. Anal. Calcd for $C_{86}H_{74}Cl_4F_6O_6P_4Ru_2S_2Se_2$: C, 51.44; H, 3.68; Se, 7.86. Found: C, 51.31; H, 3.65; Se, 10.98. FABMS (positive ion, ^{102}Ru, ^{80}Se, m/z): 1542 ($Cp_2Ru_2(PPh_3)_4Se_2^+$), 1280 ($Cp_2Ru_2(PPh_3)_3Se_2^+$), 953 ($CpRu_2(PPh_3)_2Se_2^+$), 936 ($Cp_2Ru_2(PPh_3)_2Se^+$), 920 ($Cp_2Ru_2(PPh_3)_4Se_2(OTf)_2^{2+}$), 845 ($Cp_2Ru_2(PPh_3)_4Se_4(OTf)^{2+}$), 771 ($CpRu(PPh_3)_2Se^+$), 691 ($CpRu(PPh_3)_2^+$), 509 ($Cp_2Ru_2(PPh_3)_2Se_2^{2+}$). UV/vis ($CH_2Cl_2$): 790 nm ($\epsilon = 8.18 \times 10^3$ M^{-1} cm^{-1}), 480 (sh), 370 (sh).

Attempted Reaction of $[CpRu(PPh_3)_2]_2Se_2(OTf)$ with H_2. A solution of $[CpRu(PPh_3)_2]_2Se_2(OTf)_2$ in CD_2Cl_2 (NMR tube) was purged with H_2. After 40 min, the ^1H NMR spectrum showed no change.

$[(MeCp)Ru(PPh_3)]_2Se_4(OTf)_2$ (2). Solid AgOTf, 0.22 g (0.85 mmol), was added to a solution of 0.52 g (0.7 mmol) of $(MeCp)Ru(PPh_3)_2Cl$ in 20 mL of CH_2Cl_2, and the slurry was stirred for 3 h. Excess Se, 0.44 g (5.6 mmol), was added to the filtered solution, and the mixture was stirred for ca. 24 h. After filtration, the black residue was extracted with ca. 50 mL of acetone. The red-brown extract was concentrated to ca. 5 mL and diluted with ether, giving a red-brown precipitate. This product was collected, washed with ether, and dried in vacuo. Yield: 0.42 g (0.28 mmol, 80%). Anal. Calcd for $C_{50}H_{44}F_6O_6P_2Ru_2S_2Se_4$: C, 40.05; H, 2.94; Se, 21.09. Found: C, 40.18; H, 3.02; Se, 21.11. ^1H NMR (CD_3CN): 7.67 (m, 30 H), 5.67 (m, 2 H), 4.77 (m, 4 H), 4.24 (m, 2 H), 1.14 ppm (s, 6 H). The multiplets (m) for the C_5H_4Me signals appear as slightly broadened singlets. $^{31}P\{^1H\}$ NMR (CH_3CN/acetone-d_6): 31.28 ppm. FABMS (positive ion, ^{101}Ru, ^{79}Se, m/z): 1200 ($(MeCp)_2Ru_2(PPh_3)_2Se_4^+$), 1121 ($(MeCp)_2Ru_2(PPh_3)_2Se_3^+$), 859 ($(MeCp)Ru_2(PPh_3)Se_4^+$), 780 ($(MeCp)Ru_2(PPh_3)Se_3^+$), 679 ($(MeCp)Ru(PPh_3)Se_2^+$), 600 ($(MeCp)Ru(PPh_3)Se_2^{2+}$), 521 ($(MeCp)Ru(PPh_3)Se^+$), 442 ($(MeCp)Ru(PPh_3)^+$). UV/vis ($CH_2Cl_2$): 515 nm ($\epsilon = 2.2 \times 10^3$ M^{-1} cm^{-1}) 430 (w, sh), 390 (w, sh). The cyclic voltammogram of **2** in CH_3CN shows two overlapping reversible reduction waves centered at 360 and 195 mV and a quasi-reversible wave at −1100 mV. The reduction waves at 360 and 195 mV are assigned to the reduction of **2** to neutral $[(MeCp)Ru(PPh_3)]_2Se_4$.

Conversion of $[CpRu(PPh_3)_2]_2Se_2(OTf)_2$ to $[CpRu(PPh_3)]_2Se_4(OTf)_2$. To a solution of 0.050 g (0.027 mmol) of **1** in 50 mL of CH_2Cl_2 was added 0.30 g (0.475 mmol) of red selenium. The resulting slurry was heated to reflux for 20 h, during which time the color of the solution changed from yellow-brown to pale red. The mixture was cooled to room temperature and filtered in air, leaving a black precipitate. The black solid was washed with CH_3CN (3 × 20 mL), and the red-brown extract was combined with the filtrate. The resulting red-brown solution was concentrated to 10 mL and the product precipitated by the addition of 40 mL of diethyl ether. The product was collected by filtration and dried. Yield: 0.030 g (76%). ^1H NMR (CD_3CN): 7.5–8.0 (m, 30 H), 4.99 ppm (s, 10 H).

$[(MeCp)Ru(PPh_3)]_2Se_4$ and Its Oxidation to 2. A solution of 0.2 g (0.133 mmol) of **2** in 20 mL of CH_3CN was treated with a solution of 0.05 g (0.26 mmol) of Cp_2Co in 10 mL of CH_3CN to give an immediate green precipitate. This slurry was stirred for 1 h and filtered. The

---

(49) KSeCN was formed in situ by reaction of a slurry of gray selenium with 1.3 equiv of KCN in $MeOH/H_2O$ (1:2) for 20 h at ambient temperature. The resulting solution was then filtered and placed in a three-necked flask fitted with a stopper, a pressure-equalized addition funnel, and a gas adapter. The solution of KSeCN was acidified by dropwise addition of 1.3 equiv (based on gray Se) of concentrated HCl over 40 min. The resulting slurry of red selenium was filtered, and the solid was washed with H_2O and CH_3OH and then dried. Yield: ~85%. *Caution!* This procedure evolves HCN. The HCN gas was removed by passing a continuous purge of air through the reaction solution during the HCl addition. The exiting gas was scrubbed by passing it through two consecutive aqueous NaOH solutions.

(50) Klayman, D. L.; Griffin, T. S. *J. Am. Chem. Soc.* **1973**, *95*, 197.

Table III. Crystal and Experimental Data

formula	Ru$_2$Se$_2$Cl$_2$S$_2$P$_4$F$_6$O$_6$C$_{92}$H$_{80}$	Ru$_2$Se$_4$S$_2$P$_2$F$_6$O$_6$C$_{50}$H$_{44}$
crystal system	monoclinic	triclinic
space group	$P2_1$	$P\bar{1}$
a, Å	15.965 (3)	10.909 (5)
b, Å	15.898 (5)	13.530 (5)
c, Å	18.406 (4)	10.064 (4)
V, Å^3	4353 (3)	1289 (2)
Z	2	1
		110.13 (3)
β, deg	111.28 (2)	112.18 (3)
γ, deg	90	79.62 (3)
density (calc), g/cm^3	1.537	1.931
diffractometer	Enraf-Nonius CAD4 automated κ-axis diffractometer	Enraf-Nonius CAD4 automated κ-axis diffractometer
μ, cm^{-1}	14, 12	35.78
transm factor range (numerical)	0.946–0.739	0.690–0.489
2θ limit, deg (octants)	48 ($\pm h,-k,+l$)	46 ($+h,\pm k,\pm l$)
no. of intensities (unique, R_i)	7508 (7098, 0.018)	3868 (3565, 0.018)
no. of intensities ($I > 2.58\ \sigma(I)$)	5379	2487
R^a	0.054	0.050
$R_w{}^b$	0.061	0.058
final difference Fourier data	$+0.98 > e/\text{Å}^3 > -0.58$	$+1.33 > e/\text{Å}^3 > -1.17$

$^a R = \sum||F_o| - |F_c||/\sum|F_o|$. $^b R_w = (\sum w(|F_o| - |F_c|)^2/\sum w|F_o|^2)^{1/2}$.

product was washed with CH$_3$CN and ether and dried in vacuo. Yield: 0.8 g (0.067 mmol, 45%). ^{1}H NMR (CD$_2$Cl$_2$): 7.3–7.8 (m, 30 H), 3.77 (s, 2 H), 3.35 (s, 2 H), 1.33 ppm (s, 3 H).

A solution of 0.027 g (0.08 mmol) of (C$_6$H$_5$)$_3$CBF$_4$ was added to a stirred slurry of the aforementioned green product (0.05 g, 0.04 mmol) in 10 mL of CH$_2$Cl$_2$, giving a red-brown solution within minutes. The solution was stirred for 2 h, concentrated to ca. 2 mL, diluted with hexanes, and stored at −10 °C overnight to give 0.025 g of a red-brown microcrystalline compound identified as **2** by its ^{1}H NMR spectrum.

Conversion of [(MeCp)Ru(PPh$_3$)]$_2$Se$_4$ to (MeCp)$_4$Ru$_4$Se$_4$. A slurry of 0.06 g (0.050 mmol) of [(MeCp)Ru(PPh$_3$)]$_2$Se$_4$ in 10 mL of toluene was refluxed for 4 h to give a red-brown solution. The solution was then evaporated to dryness. The ^{1}H NMR spectrum of the residue showed resonances corresponding to SePPh$_3$ and (MeCp)$_4$Ru$_4$Se$_4$. A toluene solution of the residue was chromatographed on Bio-Beads S-X4 by eluting with toluene. The brown band was concentrated to ca. 2 mL and diluted with hexanes to give 0.010 g of crystals identified as (MeCp)$_4$Ru$_4$Se$_4$[14d] by ^{1}H NMR spectroscopy.

X-ray Crystallography. [CpRu(PPh$_3$)$_2$]Se$_2$(OTf)$_2$. The orange, translucent, platy crystals of **1**·CH$_2$Cl$_2$·PhMe used for data collecting had well-developed faces. There were no crystallites or other contaminating substances on the surface of the sample. The crystal was bound by the following inversion-related forms: {001}, {100}, {010}. Distances from the crystal center to these facial boundaries were 0.02, 0.10, and 0.35 mm, respectively. The crystal was mounted under inert atmospheric conditions with the (0$\bar{1}$0) scattering planes roughly normal to the spindle axis. Data were collected at −25 °C. No problems were encountered in collecting the data, and there was no change in the appearance of the sample during the experiment.

The structure was solved by direct methods (SHELXS-86); correct positions for the ruthenium, selenium, and phosphorus atoms were deduced from an E map. Subsequent least-squares difference Fourier calculations gave positions for the remaining non-hydrogen atoms, which included methylene chloride and toluene solvate molecules. Contributions from hydrogen atoms were not included in structure factor calculations. In the final cycle of least squares, isotropic thermal coefficients were refined for the fluorine, oxygen, and carbon atoms, and anisotropic thermal coefficients were refined for the remaining atoms. Successful convergence was indicated by the maximum shift/error for the last cycle. Anisotropic thermal coefficients for the chlorine atoms converged to abnormally high values, probably indicating disorder or partial occupancy. The final difference Fourier map suggested that the oxygen and fluorine positions of the second triflate may have been rotationally disordered and that the methyl carbon atom of the toluene was disordered in two positions. A final analysis of variance between observed and calculated structure factor amplitudes and inverse sin θ showed no apparent systematic errors. Atomic coordinates are presented in Table IV.

[(MeCp)Ru(PPh$_3$)]$_2$Se$_4$(OTf)$_2$. The opaque, red, prismatic crystal used for data collection had well-developed faces. The ($\bar{1}1\bar{3}$) face was damaged. There were no crystallites or other contaminating substances on the surface of the crystal. The crystal was bound by the following forms: {001}, {010}, {100}, and face ($\bar{1}1\bar{3}$). Distances from the crystal center to these facial boundaries were 0.06, 0.07, 0.14, and 0.06 mm, respectively. Epoxy was used to mount the crystal on a thin glass fiber with the (3$\bar{3}$2) scattering planes roughly normal to the spindle axis. No problems were encountered during data collection, and there was no change in the appearance of the sample during the experiment.

Table IV. Atomic Coordinates for [CpRu(PPh$_3$)$_2$]Se$_2$(OTf)$_2$·CH$_2$Cl$_2$·PhMe

	x/a	y/b	z/c
Ru1	0.91982 (7)	0.3733	0.81272 (6)
Ru2	1.17434 (7)	0.09282 (9)	0.86765 (6)
Se1	0.97254 (8)	0.2378 (1)	0.80383 (8)
Se2	1.12327 (8)	0.2331 (1)	0.83425 (8)
P1	0.8866 (2)	0.4265 (2)	0.6842 (2)
P2	0.7799 (2)	0.3094 (2)	0.7908 (2)
P3	1.3196 (3)	0.1494 (3)	0.9069 (2)
P4	1.1500 (3)	0.0486 (2)	0.7388 (2)
C1	1.0092 (9)	0.3851 (10)	0.9371 (8)
C2	0.9235 (10)	0.4201 (10)	0.9278 (9)
C3	0.9100 (9)	0.4906 (9)	0.8770 (8)
C4	0.9879 (9)	0.4986 (9)	0.8562 (8)
C5	1.0490 (9)	0.4331 (10)	0.8918 (8)
C6	1.1362 (9)	0.077 (1)	0.9738 (8)
C7	1.0638 (9)	0.0459 (9)	0.9073 (8)
C8	1.0952 (9)	−0.0213 (9)	0.8774 (8)
C9	1.1898 (9)	−0.0359 (9)	0.9218 (8)
C41	0.7924 (6)	0.2068 (5)	0.8413 (5)
C51	0.7059 (5)	0.3709 (6)	0.8262 (5)
C61	0.7055 (5)	0.2813 (6)	0.6922 (4)
C71	1.4122 (6)	0.0817 (6)	0.9059 (6)
C81	1.3359 (6)	0.2472 (5)	0.8605 (5)
C91	1.3581 (6)	0.1812 (6)	1.0101 (4)

Table V. Atomic Coordinates for [(MeCp)Ru(PPh$_3$)]$_2$(μ-Se$_2$)$_2$(OTf)$_2$

	x/a	y/b	z/c
Ru	0.37094 (9)	0.44031 (7)	0.0407 (1)
Se1	0.4709 (1)	0.41059 (8)	−0.1543 (1)
Se2	0.5817 (1)	0.45878 (9)	0.2648 (1)
P	0.4326 (3)	0.2567 (2)	0.0175 (3)
C1	0.227 (1)	0.5045 (9)	0.171 (1)
C2	0.184 (1)	0.4077 (9)	0.058 (1)
C3	0.159 (1)	0.4177 (9)	−0.087 (1)
C4	0.185 (1)	0.5211 (10)	−0.065 (1)
C5	0.224 (1)	0.5755 (9)	0.091 (1)
C6	0.250 (1)	0.534 (1)	0.333 (1)
C7	0.292 (1)	0.1751 (8)	−0.089 (1)
C13	0.504 (1)	0.2294 (8)	0.199 (1)
C19	0.553 (1)	0.1902 (8)	−0.075 (1)

The structure was solved by direct methods (SHELX-86); correct positions for the three independent metal atoms were deduced from an E map. A weighted difference Fourier calculation revealed positions for all non-hydrogen atoms of the cation. Subsequent least-squares difference Fourier calculations revealed three disordered positions for the anion. Hydrogen atoms were included as fixed contributors in idealized positions. In the final cycle of least squares, anisotropic thermal coefficients were refined for non-hydrogen cation atoms, and group isotropic thermal parameters were varied for the anion and hydrogen atoms. The triflate was refined as three rigid groups with the site occupancy of each independently varied.[51] Successful convergence was indicated by the maximum shift/error for the last cycle. The highest residual electron density located in the final difference Fourier map was in the vicinity of the disordered triflate molecule. A final analysis of variance between observed and calculated structure factors showed no apparent systematic errors. Atomic coordinates are presented in Table V.

Acknowledgment. This research was supported by the National Science Foundation.

Registry No. **1**, 139584-16-0; **1**·CH_2Cl_2·PhMe, 139584-23-9; **2**, 139584-18-2; $CpRu(PPh_3)_2SeH$, 139606-50-1; $CpRu(PPh_3)_2Cl$, 32993-05-8; $(Me_4N)SeH$, 139584-19-3; $(MeCp)Ru(PPh_3)_2SeH$, 124858-03-3; $(MeCp)Ru(PPh_3)_2Cl$, 55272-36-1; $[CpRu(PPh_3)]_2Se_4(OTf)_2$, 139584-21-7; $[(MeCp)Ru(PPh_3)]_2Se_4$, 139584-22-8; $(MeCp)_4Ru_4Se_4$, 124858-08-8; $(C_6H_5)_3CBF_4$, 341-02-6.

Supplementary Material Available: For **1** and **2**, tables of thermal parameters, complete positional parameters, bond angles, and bond distances (18 pages); tables of structure factors (47 pages). Ordering information is given on any current masthead page.

---

(51) CSD entry TFMSUL (oxonium trifluoromethanesulfonate): Spencer, J. B.; Lundgren, J. O. *Acta Crystallogr.* **1973**, *B29*, 1923.

Contribution from the Department of Chemistry,
Texas A&M University, College Station, Texas 77843-3255

Semilocalized Bonding Schemes in Extended Systems: Orbital Localization in Y_2Cl_3 and Interstitial Derivatives

Kyeong Ae Yee and Timothy Hughbanks*

Received September 5, 1991

A semilocalized description of bonding in extended metal–metal-bonded systems is described for the prototype title compounds. Beginning with calculated band orbitals, we explicitly construct localized orbitals (Wannier functions) for the metal–metal-bonding orbitals of a M_6X_{12} cluster and the Y_2Cl_3 chain compound. Face-localized three-center bond orbitals for a Zr_6Cl_{18} cluster are remarkably similar to the HOMO for a $(Zr_6Cl_{12}H_7)Cl_6^{3-}$ cluster in which hydrogens cap seven of eight Zr_6 cluster faces. The $(Zr_6Cl_{12}H_7)Cl_6^{3-}$ cluster was chosen to model $(Th_6Br^i{}_{12}H_7)Br^{a-a}{}_{6/2}$, reported recently by Simon and co-workers. A semilocalized bonding picture for semiconductors with the Gd_2Cl_3 structure type is constructed, providing clarification of both structure–property relationships and trends in interstitial chemistry of these compounds. For the metal–metal bonding, a scheme with two 4c–2e bonds and one 2c–2e bond per cell is extracted from the band structure. The insertion of hydrogens into the tetrahedral interstices of these chains (to form structures of the β-Y_2Cl_3N type) is seen to be plausible and chains formulated as $Y_4Cl_6H_2^{2+}$ are electronically viable.

Introduction

Local Orbitals for Clusters. There are several reasons for the difficulty with which molecular and solid-state inorganic chemists have difficulty communicating. Among the most important of these is the more practiced eye of the solid-state chemists in recognizing the order within extended solid-state structures. But this advantage is often negated by the lack of even qualitatively correct ways of describing bonding in solids within a localized framework. There are a number of reasons for pursuing useful local bonding representations, among them are (i) to offer experimentalists more guidance than is generally given by computational theory. Explanations for materials' properties that boil down to statements which assure us that "its in the band structure" are at best useful only for particular compounds for which computations have been carried out. Uncovering a localized description in the electronic structure can greatly aid in analyzing structurally similar materials and therefore aid in formulating synthetic goals. (ii) Local descriptions will provide a way for chemists to recognize *explicit* structure–property relationships that are a crucial prerequisite if we are to develop the ability to control properties. (iii) Understanding of the structural and reaction chemistry of the solids under investigation will inevitably be enhanced. Chemistry deals with inherently local phenomena; bonds are clearly made and broken *locally*. If appropriate analogies are to be drawn with the chemistry of molecules, then we must be able to compare the local electronic structure of molecules and solids.

Cluster compounds can serve to illustrate a way in which localized bonding can be extracted from delocalized representations. It has been known for some time that metal–metal bonding in octahedral clusters such as $Nb_6Cl_{12}^{2+}$ and $Mo_6Cl_8^{4+}$, in which nonmetals respectively cap the octahedron's edges and faces, could be understood using localized orbitals.[1] In the latter case 12 metal-based electron pairs may be viewed as localized in 2c–2e bonds along the octahedral edges, and in the former case the cluster's 16 Nb–Nb bonding electrons occupy localized 3c–2e bonds in the eight cluster faces. The power of the localized bonding view is underlined by the recent synthesis of the remarkable compound $Th_6Br_{15}H_7$ (**1**).[2,3a] The clusters in this compound form a body-centered cubic array as in the Nb_6F_{15} structure type; $[(Th_6H_7)Br^i{}_{12}]^{3+}$ clusters are linked via linear

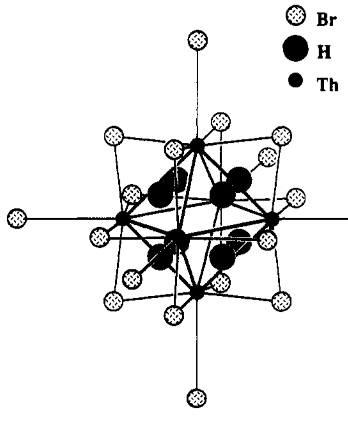

1

---

[*] To whom correspondence should be addressed.

(1) Kettle, S. F. A. *Theor. Chim. Acta* **1965**, *3*, 211.

(2) (a) Simon, A.; Böttcher, F.; Cockcroft, J. K. *Angew. Chem., Int. Ed. Engl.* **1991**, *30*, 101. (b) Böttcher, F.; Simon, A.; Kremer, R.; Buchkremer-Hermanns, H.; Cockroft, J. *Z. Anorg. Allg. Chem.* **1991**, *598/599*, 25.

(3) (a) Andersen, O. K. Cited in reference 2a. (b) Andersen, O. K.; Satpathy, S. *Basic Properties of Binary Oxides*; University of Seville: Seville, Spain, 1983.